

# Fluid-structure interaction for water hammers effects in petroleum and nuclear plants

**R. Messahel<sup>1,2</sup>, B. Cohen<sup>3</sup>, M. Souli<sup>1</sup>, M. Moatammedi<sup>2</sup>**

<sup>1</sup>USTL Lille 1, Cité Scientifique, 59655, Villeneuve Cedex, France

<sup>2</sup>Narvik University College, Lodve Longesgt. 2 Postboks  
385 8505, Narvik, Norway

<sup>3</sup>EDF UTO, 6 avenue Montaigne, 93160, Noisy Le-Grand, France  
ramzi.messahel@ed.univ-lille1.fr; bernard.cohen@edf.fr;  
mhamed.souli@univ-lille1.fr; moji@hin.no

## **ABSTRACT**

Fluid-Structure Interaction (FSI) becomes more and more the focus of computational engineering in Petroleum and Nuclear Industry in the last years.

These problems are computer time consuming and require new stable and accurate coupling algorithms to be solved. For the last decades, the new development of coupling algorithms, and the increasing of computer performance have allowed to solve some of these problems and some more physical applications that has not been accessible in the past; in the future this trend is supposed to continue to take into account more realistic problem.

In this presentation, numerical simulation using FSI capabilities in LS-DYNA, of hydrodynamic ram pressure effect occurring in nuclear industry is presented.

## **1. INTRODUCTION**

Water Hammers (WHs) are hydraulic transient phenomena. They occur when we modify locally the flow conditions (pump start-up or stop, valve closure) of a fluid contained in a pipe. A shock is generated and is expressed by the discontinuity of the fluid variables (pressure, fluid velocity).

The pipe's elasticity and the fluid's compressibility propagate the shock at high velocity, giving birth to a pressure wave known as the so-called "Water Hammer".

WHs can be encountered in domestic plumbing. It is produced when machines, such as a dishwasher or a washing machine shut off the water flow. It is characterized by a loud banging sound.

In the nuclear power plants, such water hammer occurs in water supply pipes. Due to the high energy and the quantity of water in motion, there is a real threat to the nuclear safety. It can be violent and can cause several damages (plasticity of pipes and even the rupture of brackets supporting pipes) to the structure. Those fast dynamic phenomena are of the order of  $1e-4$  seconds in time, and the actual sensors on nuclear power plants are not accurate enough to capture the pressure wave. Numerical solution can help having a better understanding of those rapid dynamic transients. Simulation of such phenomena is computer time consuming and requires stable and accurate coupling algorithms. Using FSI capabilities of LS-DYNA, we present in this paper numerical simulation of hydrodynamic ram pressure effect occurring in nuclear industry.

## 2. WATER HAMMER'S THEORY

The WH with column separation, also called “the classic WH”, has always been in the heart of the research on WHs. Simpson is one of the early pioneers who worked actively on the experimentation of those phenomena. We will simulate the “Simpson’s experience” [2] performed in 1986 on the classic WH which provides a good validation case. It contains a complex physic to be modeled: Shock wave propagation, Cavitation and Fluid-Structure Interaction.

Joukowsky and Allievi gave the basis on WH’s classical theory through theoretical analysis. The rise of pressure is given by the Joukowsky’s equation

$$\Delta P = \frac{c_L \Delta V}{g}, \quad (1)$$

where  $c_L$  is the pressure’s wave speed,  $\Delta P$  is the change of pressure,  $\Delta V$  is the change of the fluid’s velocity and  $g$  is the gravitational acceleration.

The wave speed is estimated from Korteweg’s equation

$$c_L = \sqrt{\frac{K / \rho}{1 + (K / E)(D / e)}}, \quad (2)$$

where  $K$  is the bulk modulus,  $\rho$  is the mass density,  $E$  is the Young’s modulus of the pipe wall material,  $D$  is the inner diameter and  $e$  is the wall thickness.

In this paper, we define by  $\tau$  the time period for a pressure wave to travel back and forth between the valve and the reservoir.

$$\tau = \frac{2L}{c_L} \quad (3)$$

We assume a prescribed velocity at the closed valve as well as a pressure boundary condition at outlet of the reservoir. Thus according to Eqn. (1), the change in pressure always occurs at the closed valve, and the change in velocity always occurs at the reservoir.

Let us denote by  $P_r$  the pressure in the reservoir,  $P_0 = P_r$  the initial pressure,  $V_0$  the initial velocity and  $t_0$  the valve closure time.

At time  $t = t_0$ , a pressure wave  $P = P_1 = P_0 + \Delta P$  is generated at the closed valve ( $V = 0$ ) and is propagated from the valve to the reservoir at the wave propagating velocity  $c_L$ .

According to the Eqn. (1), when the pressure wave reaches the reservoir at time  $t = t_0 + \frac{\tau}{2}$ , it is reflected due to the prescribed pressure at the reservoir, and thus travels from the reservoir to the valve leaving behind a water at pressure  $P = P_r$  and  $V = -V_0$  ( $V < 0$  because of the pressure gradient  $P_1 > P_r$ ).

When the pressure wave reaches back the valve at time  $t = t_0 + 2\tau$ , the confined water in the pipe is entirely at pressure  $P = P_r$ . The change of velocity ( $-V_0$  to 0) generates a pressure drop in the cylinder at the reservoir location maintained at constant pressure  $P_r$ , the pressure drop  $\Delta P$  is given by:

$$P = P_2 = P_r - \Delta P.$$

Recalling that  $P_0 = P_r$ , thus we have  $P_2 < P_0$ . It leads us to two possible scenarios:

**Case 1:**  $P_2 > P_{sat}$

At time  $t = t_0 + \frac{3\tau}{2}$ , the pressure wave reaches the reservoir and is once again reflected to the valve. This time  $V = V_2 = V_0$  ( $V_2 > 0$ , because  $P_r > P_2$ ).

The pressure wave  $P = P_r$  reaches the valve at time  $t = t_0 + 2\tau$ . The entire water is at pressure  $P = P_r$ , and the new overpressure is  $P = P_r + \Delta P_1$ . It takes us back to the previous step at time  $t = t_0 + \tau$ , and thus we have a periodical cycle.

**Case 2:**  $P_2 < P_{sat}$

The pressure at the valve drops to the water vapor pressure. And the new pressure wave is propagated at the liquid vapor pressure.

In order to use Eqn. (1) we need to know the new wave propagation velocity depending on the vapor/water mixture.

To go further in the analytical study, we will add the two following hypothesis as it is suggested by [4]:

- Only a vapor pocket at the valve is formed during the propagation of the pressure wave from the valve to the reservoir. And we suppose that the size of the vapor pocket is very small compare to the pipe s length.
- The vapor pocket will impose its pressure to the pressure wave as the reservoir does and will act as a fixed pressure boundary condition.

Including the two previous hypothesis, we are able to use Eqn. (1). Contrary to the previous case, the reversed direction velocity is no more imposed to be zero but decreases to (Mostowsky 1929)

$$V_0 - \Delta V_{vc} = V_0 - \frac{g(P_r + P_{sat})}{a}, \tag{4}$$

Now we have a system of two reservoirs (reservoir-vapor cavity). The pressure wave is reflected by the vapor cavity until the vapor pocket collapses a time  $t = t_1$ , accelerating the water that will impact the valve and give birth to a new WH. The new rise of pressure is less than the first one, but the superposed pressure waves give a greater rise of pressure. In the Figure 1c, the superposition of pressures occurs at time  $t = t_0 + 3\tau$ .

**3. NUMERICAL SIMULATION**

Based on the Simpson’s experience [2] and a benchmark proposed by the WAHA code [5], we will present three simulations, made on LS-DYNA, of the dispositive drawn in Figure 1a.

A first one dimensional simulation will be performed, then a three dimensional simulation and finally a three dimensional simulation adding a valve on the top of the pipe that opens by the pressure wave, releasing water and dropping the pressure inside the pipe. Such configurations are set in nuclear power plant in order to protect the structure from high pressure increase. Table 1 resumes the different parameters of the Simpson’s experience for the two first simulations.

A reduced model will be considered for the third simulation. All simulations start at the closure of the valve.

A Lagrangian formulation with the MAT\_ELASTIC material model is used for the structure.

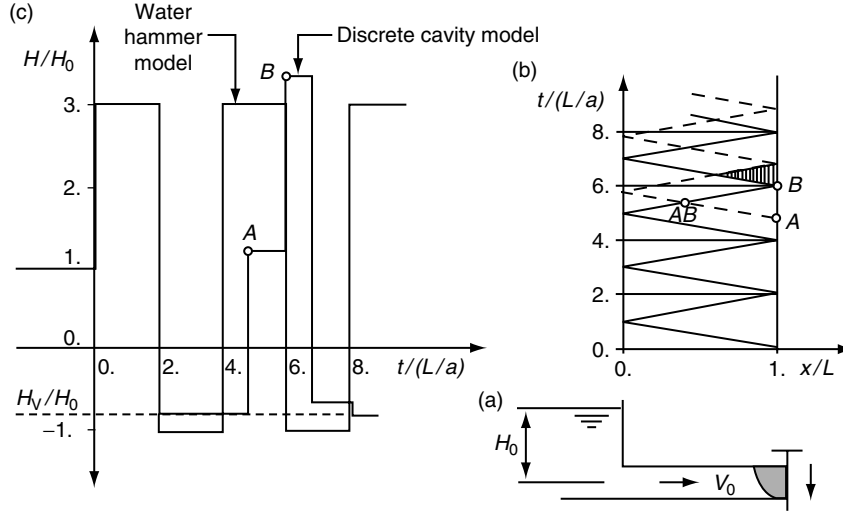


Figure 1 A short-duration pressure pulse. (a) Reservoir-pipe-valve system. (b) Wave paths in distance-time plane. (c) Piezometric head history at valve. [3].

Table 1 Simpson's Experience parameters. (a) Initial conditions. (b) Pipe's geometry and material characteristics. [2]

(a)		(b)	
Pressure (MPa)	3.419	Inside Diameter (mm)	19.05
Temperature (Degree)	23.3	Thickness (mm)	1.6
Velocity ( $\text{m}\cdot\text{s}^{-1}$ )	0.4	Elastic Modulus (Gpa)	120
		Length (m)	36

An ALE multi-material formulation will be used for the confined water in the pipe, and an ambient ALE multi-material will be used for the reservoir as an imposed pressure boundary condition. The MAT\_NULL material model is chosen for the water in both pipe and reservoir adding the linear in volume Mie-Gruneisen equation of state

$$p = \frac{\rho_0 c^2 \mu}{(1 + \mu)}, \quad \text{with} \quad \mu = \frac{\rho}{\rho_0} - 1, \quad (5)$$

where  $p$  is the pressure,  $c$  is the intercept of the  $v_s - v_p$  curve,  $\rho$  is the density,  $\rho_0$  is the initial density.

Detailed descriptions of the ALE formulation as well as the fluid-structure coupling algorithms are developed by Aquelet et al [1]. For performance CPU time, a Lagrangian coupling, where fluid nodes and structure nodes are commonly used at the fluid-structure interface, where fluid mesh is not highly distorted. In the vicinity of the opening valve, where the fluid is released out the structure tube, Eulerian coupling needs to be performed. At this location, high mesh distortion of the fluid domain can be observed, thus the classical Lagrangian formulation cannot be used without loose of accuracy due to small element Jacobian.

Table 2 MAT\_ELASTIC parameters

Pipe	RO	E	PR	DA	DB	K
	8960	1.2e + 11	0.355	0.0	0.0	0.0
	VC	CP				
	None	1.0e + 20				

RO: Mass Density, E: Young’s Modulus, PR: Poisson’s ratio, DA: Axial Damping Factor, DB: Bending damping factor, K: Bulk Modulus, VC: Tensor viscosity coefficient, CP: Cavitation Pressure.

Table 3 MAT\_NULL parameters

Water	RO	PC	MU	TEROD	CEROD	YM	PR
	997.58	-10.0	0.001	0.0	0.0	0.0	0.0

RO: Mass density, PC: Pressure cutoff, MU: Dynamic viscosity coefficient, YM: Young’s Modulus, TEROD: Relative volume for erosion in tension, CEROD: Relative volume for erosion in compression, PR: Poisson’s ration.

Table 4 Mie-Gruneisen parameters

Gruneisen	C	S <sub>1</sub>	S <sub>2</sub>	S <sub>3</sub>	Γ <sub>0</sub>	a	E <sub>0</sub>
	1492	0.0	0.0	0.0	0.0	0.0	0.0
	V <sub>0</sub>						
	0.999858						

C: Speed of sound, S<sub>i</sub> (i = 1, 2, 3): Coefficient of the slope of the v<sub>s</sub> - v<sub>p</sub> curve, Γ<sub>0</sub>: Grune sen gamma, a: the first order volume correction to Γ<sub>0</sub>, E<sub>0</sub>: Initial internal energy per unit reference volume, V<sub>0</sub>: Initial relative volume.

The different parameters are given in Table 2, Table 3 and Table 4, where the variables are expressed in the international unit system.

### 3.1. ONE DIMENSIONAL SIMULATION

Let us consider a long rectangular box made of hexahedra elements along X-axis, and two along both axis Y and Z. Recalling that LS-DYNA is a 3D code, the hint to perform a 1D simulation is to constrain the velocity on the fluid’s nodes, to follow only one direction (X-direction). Constraining the fluid’s boundary nodes, prevents the radial expansion due to the pipe’s elasticity. That is equivalent to having a “Stiff Pipe”.

In order to simulate the closed valve, we constrain all degrees of freedom (rotation and translation) of the nodes at the end of the pipe (V = 0).

The full model is composed of 67600 hexahedra elements.

### 3.2. THREE DIMENSIONAL SIMULATION

In this simulation, we consider the real geometry of the pipe. Fluid’s nodes are no more constrained and the structure is modeled by Belytschko-Tsay shell type elements. The degrees of freedom of the nodes at the end of the pipe are constrained.

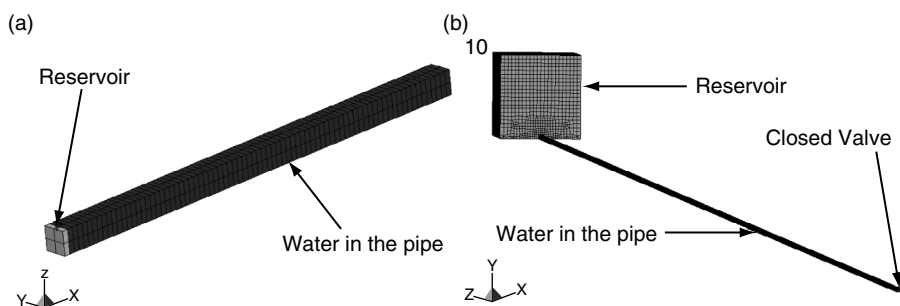


Figure 2 One dimensional model. (a) Reduced model in length. (b) Full model.

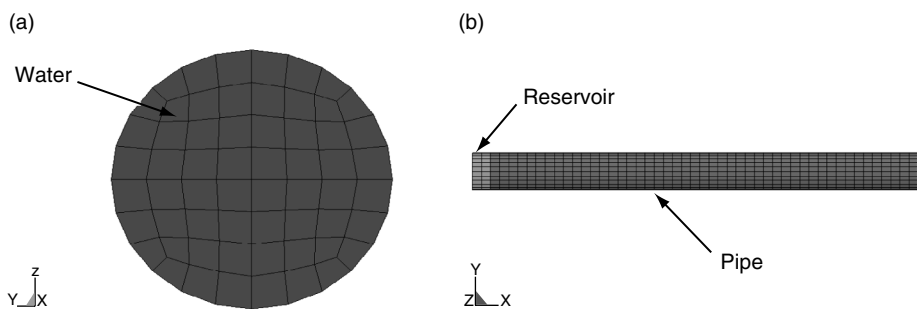


Figure 3 Reduced three dimensional model. (a) Water mesh. (b) Reservoir and pipe meshes.

We will take into account the coupling effects by merging the nodes between Lagrangian (Structure) and ALE (Fluids) parts. Common nodes of a Lagrangian and ALE mesh will be considered Lagrangian and constitute a boundary condition for the ALE mesh (material velocity = mesh velocity).

The full model is composed of 216000 hexahedra elements for the water, 120 hexahedra elements for the reservoir and 86400 four nodes shell elements for the structure.

### 3.3. THREE DIMENSIONAL WITH A VALVE SIMULATION

Considering that the two previous simulations validate the WH's modeling, we choose for this third simulation the configuration given by table 2. We start from the second simulation model, deleting structure shell elements to make the opening of the pipe and adding the valve modeled by:

- A fixed upper plate and a lower plate: Belytschko-Tsay shell type elements.
- Springs connecting the two plates: Discrete elements.
- Contacts: Upper Plate — Lower Plate and Lower Plate — Pipe.

The plate that opens due to the water pressure is embedded in an ALE mesh (Air + Water) in order to perform the Euler-Lagrange coupling, described in detail in Aquelet et al [1].

The full model is composed of 33840 hexahedra elements, 5788 four nodes shell elements and four discrete elements.

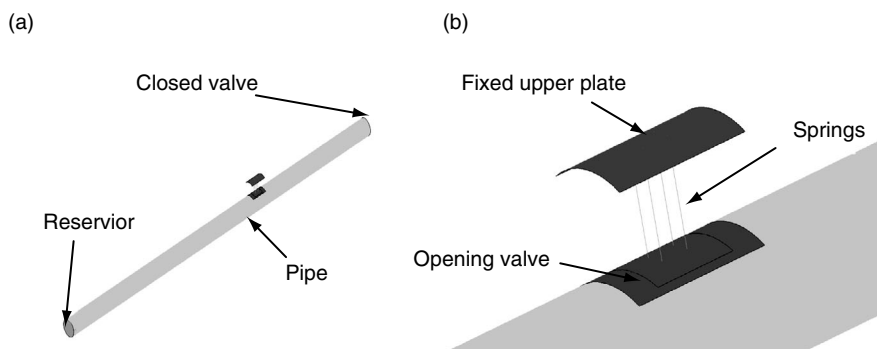


Figure 4 Three dimensional valve model. (a) Full model. (b) Zoom on the opening valve.

Table 5 Full model with the opening valve parameters. (a) Initial conditions. (b) Pipe’s geometry and material characteristics

(a)		(b)	
Pressure (MPa)	3.419	Inside Diameter (mm)	300
Temperature (Degree)	23.3	Thickness (mm)	23
Velocity (m.s <sup>-1</sup> )	0.4	Elastic Modulus (Gpa)	210
		Length (m)	12

#### 4. NUMERICAL RESULTS

The simulations are performed on a 2.0 Ghz desktop with the SMP version launched on 8 processors. The CPU time for “the one dimensional simulation”, “the three dimensional simulation” and “the three dimensional simulation including the valve” are respectively about 2 hours, 60 hours and 1 hour.

The two first simulations are compared to the experimental results and the 1D WAHA CODE benchmark results presented in figure 5 (taken from [5]). The plotted pressures are taken at the closed valve where the pressure sensors were located in the “Simpson’s experience” [2].

As shown in figure 5, the one dimensional simulation results are in good agreement with the WAHA CODE simulation using a “STIFF PIPE”. Pressure values from LS-DYNA simulation have been compared to experimental data given by [5], and good correlations have been observed, as shown in figure 5. Indeed the radial expansion of the pipe is not considered due to the stiffness of the pipe which causes an over-estimation of both the pressure and the wave propagation speed.

Figure 6 shows the pressure of the water at the middle of the pipe. In order to show the effects of the pressure on the pipe and the radial expansion, we show in figure 7 the z-displacement of two nodes located on the middle of the pipe and diametrically opposed in the XZ plan. We can remark that in absence of the pressure wave the nodes are in phase and in presence of the pressure wave the nodes displace in opposite direction but at the same amplitude.

In figures 8 is plotted the pressure in the water below the opening valve with a blocked plate (holding the water in the pipe) and a free plate (releasing the water at the opening). Comparing both graphs, we can observe a pressure release when using a free plate. This pressure release is mainly due to the opening of the valve which occurs when the pressure wave reaches the valve and applies a loading force on the plate. In our simulation this event occurs at time  $t = 0.004$  sec.

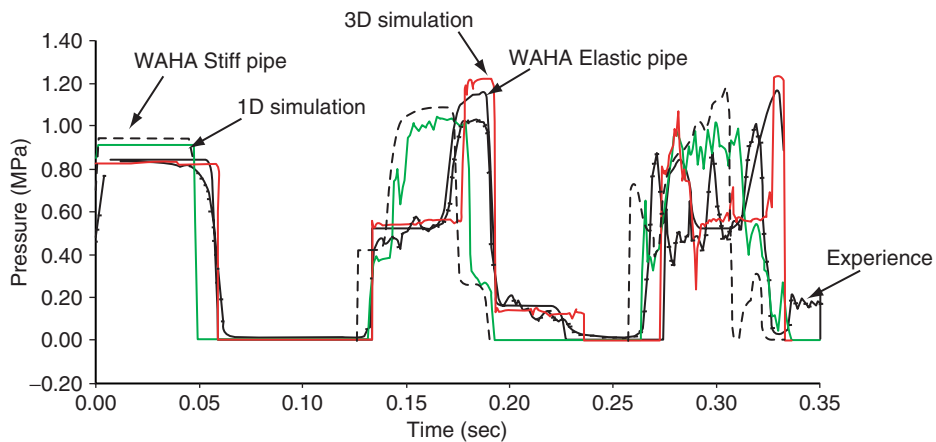


Figure 5 Pressure at the closed valve [5].

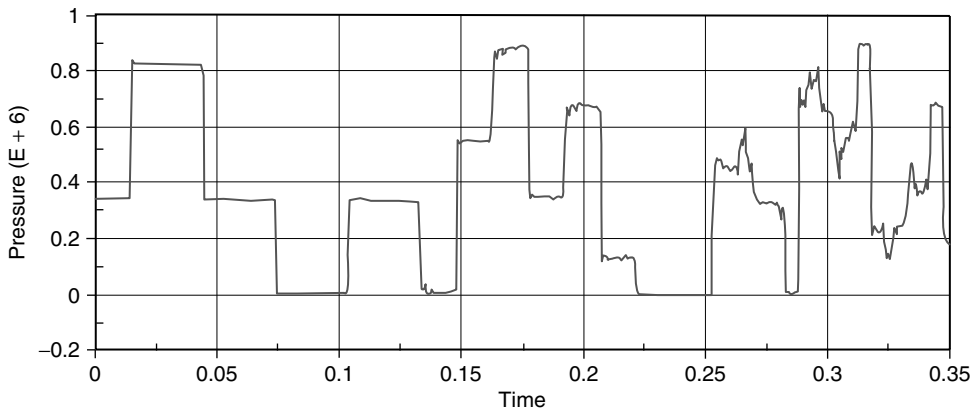


Figure 6 Water pressure at the middle of the pipe.

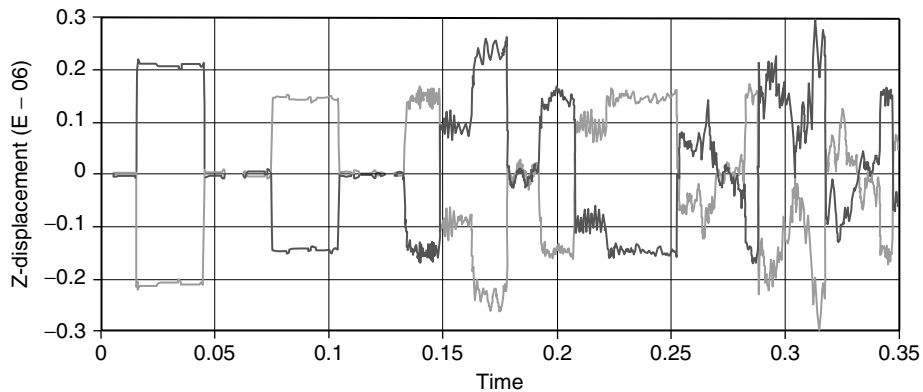


Figure 7 Z-displacement of two opposite middle pipe's node located in the XZ plan.



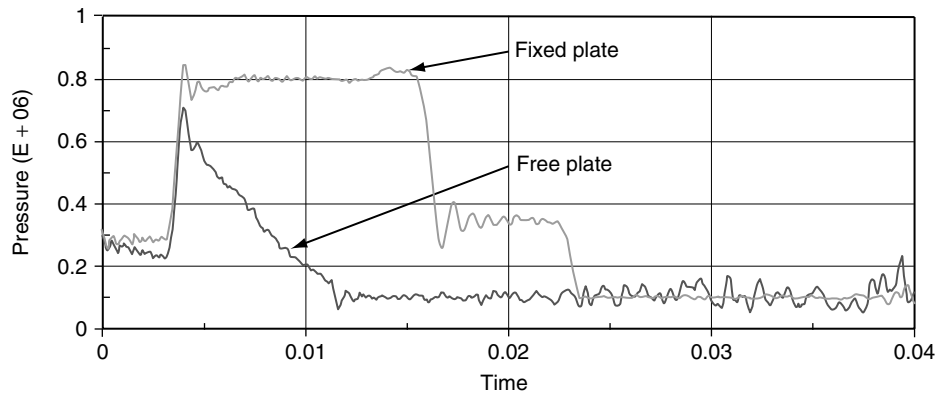


Figure 8 Pressure at location below the opening valve.

The opening effect is controlled by a spring system attached to the free plate, as shown in figure 9. The values of the spring stiffness are set empirically following literature data.

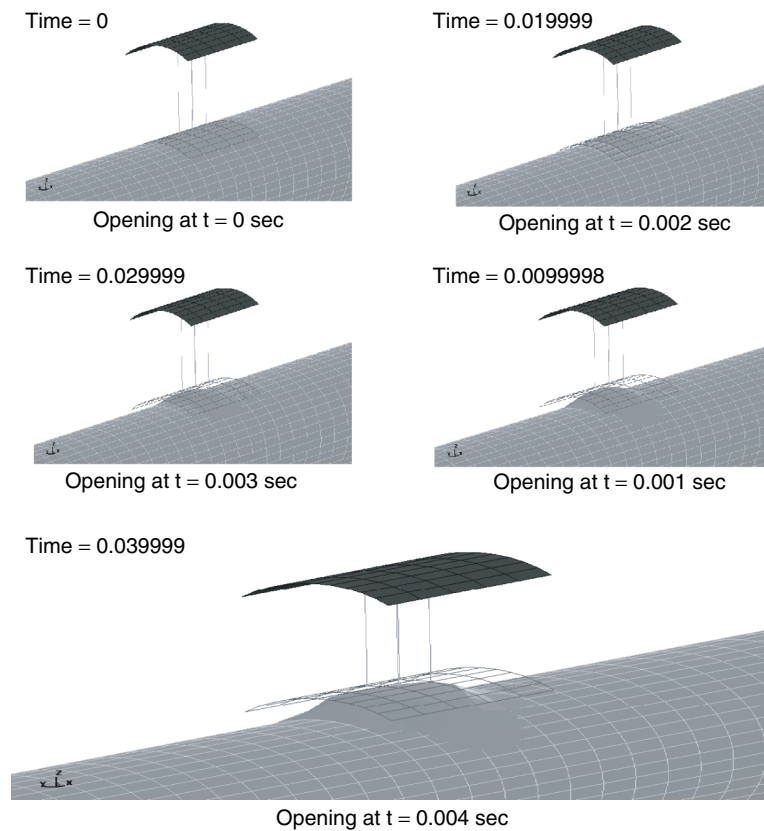


Figure 9 Dynamic opening of the valve and water release.

